Thermal modelling for on-interposer thermoelectric sensors

C. Morel[1,2] and G. Savelli[1,2]
[1] Univ. Grenoble Alpes, F-38000 Grenoble, France
[2] CEA, Liten, Nanomaterials Technologies Department, F-38000 Grenoble, France

Introduction

This paper presents a study about micro ThemoElectric-Sensors (µTES). These µTES are used to detect hot temperature spots in microelectronic devices, allowing to deliver a global thermal map identifying areas to cool. µTES are based on the Seebeck effect which converts thermal flow to electrical signals. Two thermoelectric (TE) materials have been tested in this study, namely polycrystalline SiGe (Silicium-Germanium alloy) and silicide-based Quantum Dot Super Lattices (QDSL). Our objective is to obtain a high µTES sensitivity (around 100 mV/K) with a low response time.

Experimental Set-up

Several µTES have been processed around a 5.2x5.8 mm² hot source dissipating a 3 W thermal power. Each µTES is made of several p-n junctions connected electrically in series and thermally in parallel. The p and n lines are characterized by positive S_p and negative S_n Seebeck coefficients, respectively, corresponding to a global Seebeck coefficient equal to:

$$S_{np} = S_p - S_n \tag{1}$$

The sensitivity Se of a µTES is defined by the following equation:

$$Se = \frac{V_{oc}}{\Delta T} = N \times S_{np} \tag{2}$$

where N is the number of junctions and V_{oc} the open-circuit voltage generated by the temperature difference ΔT. Here, the temperature and electric potential fields are determined by numerical calculations then the µTES sensitivity for each particular geometry is calculated.

Thermoelectric Governing Equations

The equations solved are the ones for the temperature T and the electric potential U [1]. The temperature equations are:

$$\begin{aligned} &\rho C \frac{\partial T}{\partial t} + \nabla . \underline{q} = Q \\ &\underline{q} = -k\nabla T + ST\underline{J} \\ &Q = \underline{J}.\underline{E} \qquad \underline{E} = -\nabla U \end{aligned} \tag{3}$$

where ρ denotes the material density, C the specific heat capacity and k the thermal conductivity. The heat flux density $\underline{q}$ is split in two contributions: the usual heat transfer proportional to the temperature gradient (Fourier's law) and an additional contribution due to the Seebeck effect where S is the Seebeck coefficient (measured in µV/K) and $\underline{J}$ is the electric current density (in A/m²) given by the following equation:

$$\underline{J} = -\sigma\left(\nabla U + S\nabla T\right) \tag{4}$$

where σ is the electrical conductivity (measured in S/m). In Eqs. (3), the other relevant quantities are the electric field $\underline{E}$ and the Joule heat source Q.
According to Jaegle [2] the equation for the electric potential U is:

$$\varepsilon\left[\frac{\partial^2 U}{\partial x \partial t} + \frac{\partial^2 U}{\partial y \partial t} + \frac{\partial^2 U}{\partial z \partial t}\right] = -\nabla . \underline{J} \tag{5}$$

where ε is the material permittivity.

Geometrical model

A typical µTES involves several hundred junctions, but in order to keep manageable simulations, we will only reproduce the behavior of five junctions and extrapolate the obtained sensitivity to the number of junctions of the real system. We can also reproduce several micro-channels (containing air or circulating water) under the thin layer of the simulated portion of the µTES. The simulated system is illustrated on the Figures 1-6.

Excerpt from the Proceedings of the 2017 COMSOL Conference in Rotterdam

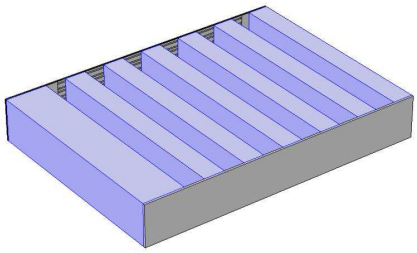

Figure 1: Bottom view of the system showing the six µchannels.

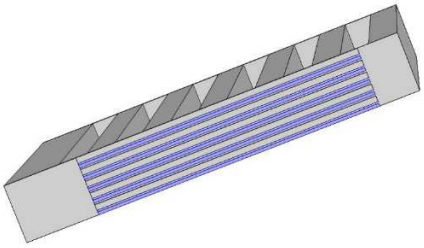

Figure 2: Top view showing the p-type TE lines in blue.

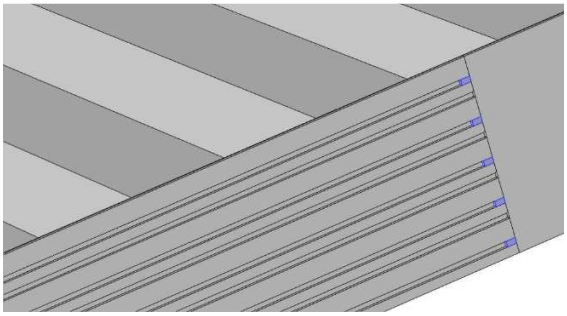

Figure 3: Zoom showing the metallic electrical connections between the p and n lines (in blue on the figure).

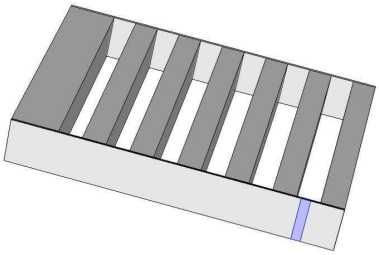

Figure 4: Hot source in blue (µchannels are also clearly visible on this figure).

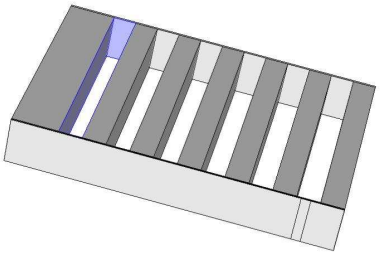

Figure 5: possible exchange with water (where the channel walls are colored in blue).

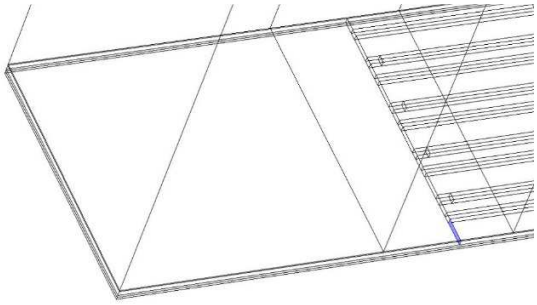

Figure 6: Ground is located at one extremity of the µTES (in blue).

A thin layer containing ten lines p and n connected electrically by small silicides are placed on a wafer of silicium oxide pierced by several rectangular channels (or not pierced). A thermal boundary condition (BC) is imposed on an aluminum part showed in figure 4. This BC can be a Dirichlet BC (the temperature is imposed equal to 120°C which is the maximum admissible temperature) or a Neumann BC (the heat flux density is imposed). If the Neumann BC is chosen, the heat flux density is calculated from the TTC characteristics: q" = P/S = 3W/(5.8*5.2 mm^2) = 99469 W/m^2.

Material properties

The material properties measured from poly-SiGe and QDSL at room temperature are given in Table 1.

Table 1: TE material properties.

property	SiGe	SiGe	QDSL	QDSL
Line type	p	n	p	n
$r = 1/\sigma$	3.10^{-5}	$3{,}4.10^{-5}$	$1{,}6.10^{-4}$	$2{,}5.10^{-4}$
S (µV/K)	142	-185	253	-267
k (W/mK)	4.7	4.1	5.3	6.3
ρ (kg/m^3)	2330	2330	2330	2330
C (J/kgK)	710	710	710	710

According to Eq. (2), the number of junctions N must be at least 306 for poly-SiGe and 193 for QDSL to obtain a sensitivity Se equal to 100 mV/K. Table 2 summarizes the geometrical parameters retained for the complete µTES.

Table 2: Geometrical parameters.

Parameters	Values
Line length	500 µm
Line thickness	2 µm
N	315
Line width	5 µm
Line spacing	3 µm
Total width	5.04 mm

Results with Dirichlet BC

Following results are obtained with poly-SiGe material, in a configuration without µchannels and a temperature equal to 120°C at the Dirichlet BC for the hot source. Figure 7 shows that the temperature obtained in the whole domain at time = 10 s is near 120°C and Figure 8 shows the surface electric potential field which gives a voltage equal to 0.9 mV.

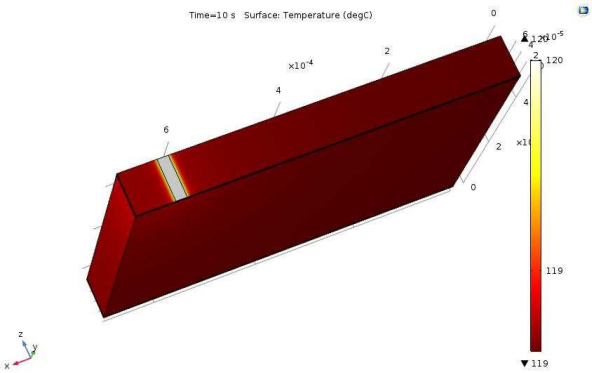

Figure 7: Temperature field at t = 10 s.

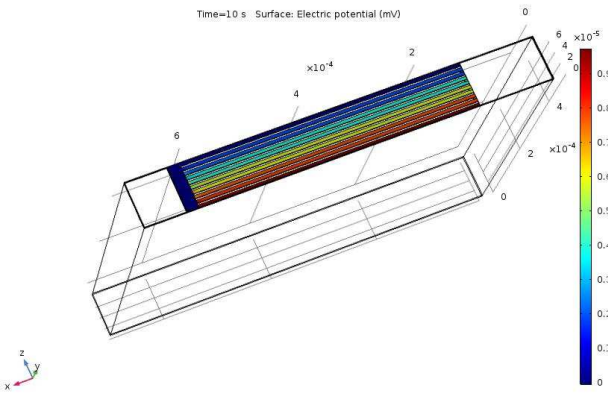

Figure 8: Potential field at t = 10 s.

This thermal equilibrium is quickly obtained and Figures 9-10 show the time evolution of the µTES temperatures at the hot and cold sides and the output voltage for the first 0.5 s.

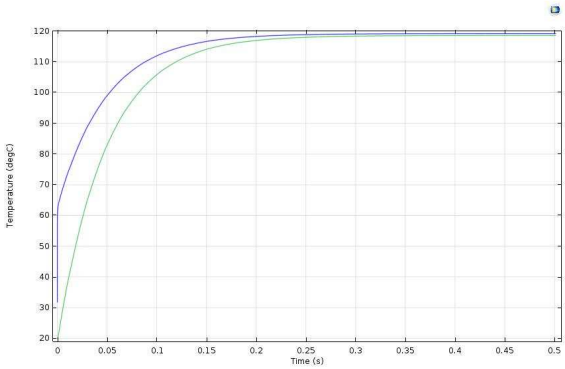

Figure 9: Temporal evolution of the hot and cold sides temperatures.

Figures 10 and 12 show that a voltage peak is achieved at the beginning of the simulation. Figures 9-10 for poly-SiGe show that this peak is equal to 70 mV and the corresponding temperature difference between the hot and cold sides is approximately equal to 43°C. Using Eq. (2), a sensitivity Se equal to 1.63 mV/°C is found for only 5 junctions. Therefore, the resulting sensitivity for a µTES having 315 junctions would be 103 mV/°C which is above the required 100 mV/°C.

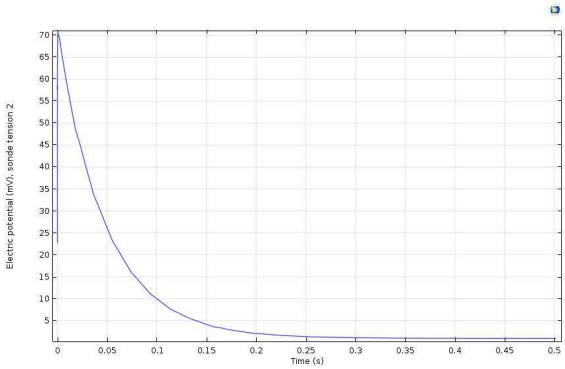

Figure 10: Temporal evolution of the output voltage.

Figures 11-12 present the same results obtained from the QDSL material.

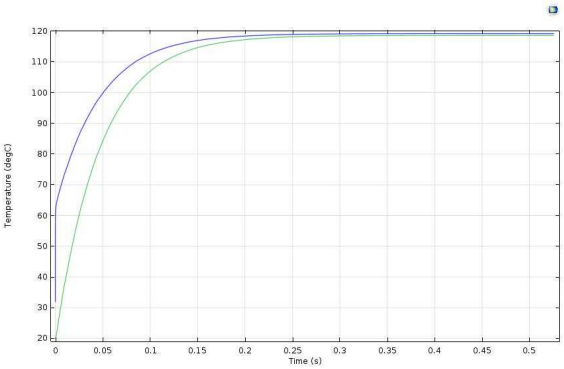

Figure 11: Hot and cold sides temperatures with QDSL.

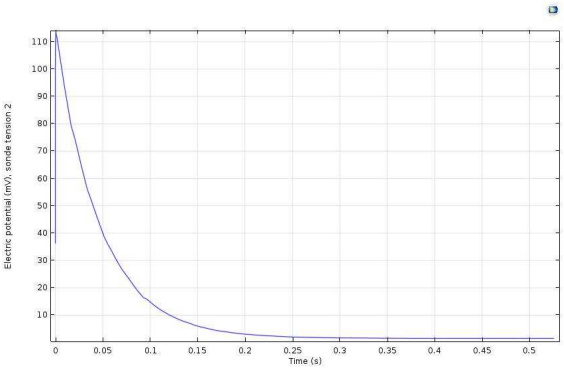

Figure 12: Output voltage with QDSL.

As shown in these figures, the temperature difference did not changed (43°C) but the voltage peak is now equal to 112 mV. Therefore, we find a sensitivity equal to 2.6 mV/°C for 5 junctions, corresponding to 164 mV/°C for 315 junctions. A QDSL-based µTES has a higher sensitivity than a poly-SiGe-based µTES due to higher Seebeck coefficient for QDSL (see Table 1).

Results with Neumann BC

Here the Dirichlet BC on the temperature is replaced by a Neumann BC, with a heat flux density equal to 99469 W/m^2. In this case, the increase of temperatures on the two sides of the µTES is quite slow (see Figure 13).

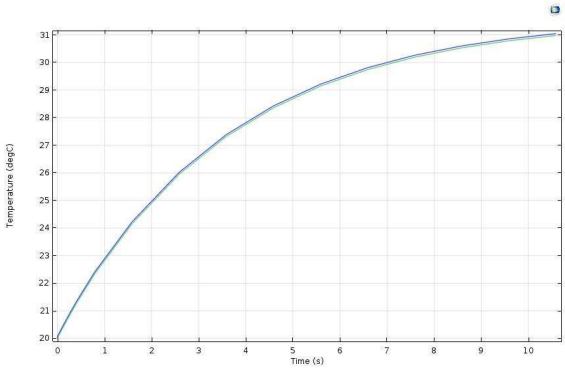

Figure 13: Temperature increase on the hot and cold sides of the µTES.

Nevertheless, if a zoom on the beginning of the calculation is made, we can see that a temperature difference between the hot and cold sides appears quickly, and then remains constant (see Figure 14).

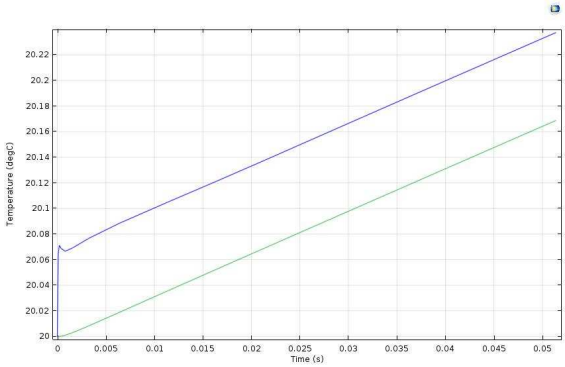

Figure 14: Zoom of the temperatures at the beginning of the calculation.

The output voltage also increases rapidly at the beginning and then remains approximately constant, as shown in Figure 15.

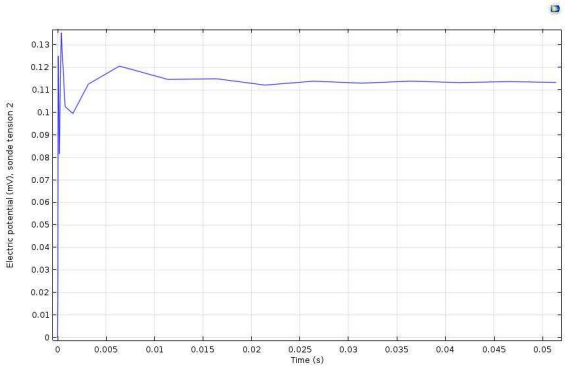

Figure 15: Output voltage with poly-SiGe.

Figure 16 represents the corresponding result obtained for QDSL material.

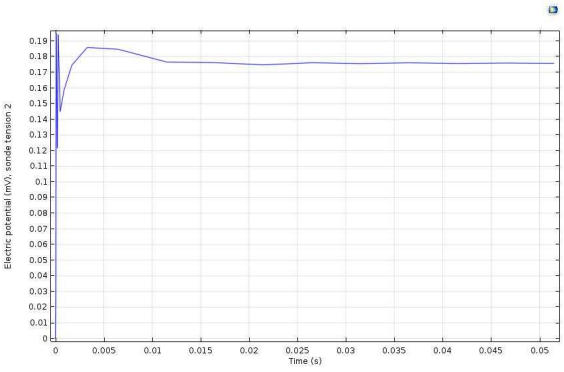

Figure 16: Output voltage with QDSL.

Here again, the voltage peak is reached very quickly, i.e. in the first milliseconds. The peak value is 0.12 mV for poly-SiGe and 0.19 mV for QDSL, with a temperature difference equal to 0.072°C. This gives a sensitivity Se = 1.66 mV/°C for poly-SiGe and 2.64 mV/°C for QDSL in the case of 5 junctions. For the real case of 315 junctions, we obtain Se = 105 mV/°C for poly-SiGe and 166 mV/°C for QDSL, still greater than the 100 mV/°C required.

Effect of the channels

In this section, µTES and micro-channels technologies are combined (see Figures 1-5). The goal is to increase the temperature difference between the two sides of the sensor. These µchannels are filled with air (exchanged coefficient equal to 15 W/m^2/°C) and the last one (the nearest from the µTES cold side) with flowing water (exchange coefficient equal to 10000 W/m^2/°C). Figure 17 shows a temperature field at time t = 10 s obtained with six channels and poly-SiGe lines. The temperature BC for this calculation is the imposed heat flux.

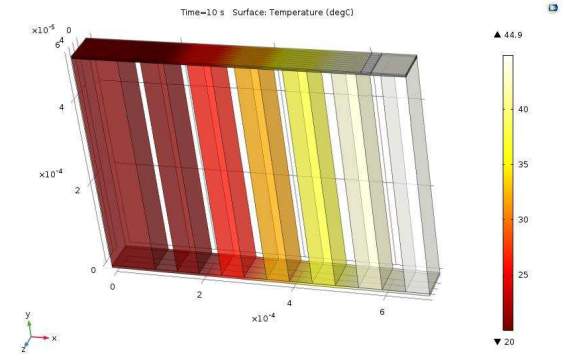

Figure 17: Temperature field with micro-channels.

Figures 18 and 19 give the two sides temperature evolution and the output voltage evolution for this calculation.

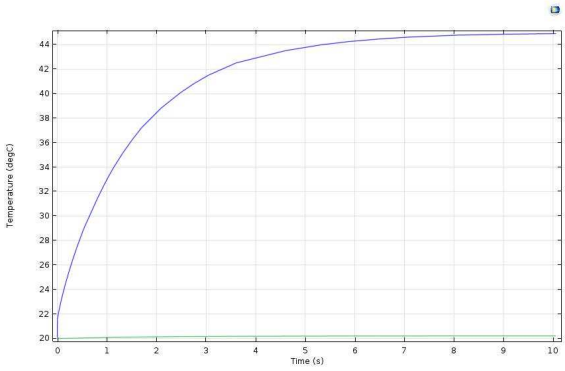

Figure 18: Temporal evolution of the hot and cold sides temperatures with micro-channels.

The effect of the micro-channels is clearly visible in this figure since the cold side remains at the initial temperature of 20°C, giving a final temperature difference around 25°C.

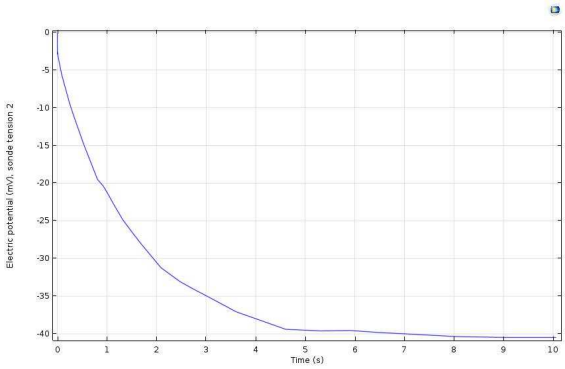

Figure 19: Time evolution of the output voltage.

The absolute value of the output voltage attains 41 mV at the end of calculation (t = 10 s), corresponding to a sensitivity of 103 mV/°C for 315 junctions.

Conclusions

In this paper, the influence of µTES geometry and TE materials has been studied thanks to COMSOL Multiphysics software. Our objective was to obtain a µTES sensitivity greater than 100 mV/°C with a fast response time. This objective has been achieved for the two types of material: poly-SiGe and QDSL, and it has been shown that the QDSL has a 60% higher sensitivity than poly-SiGe material.

Acknowledgements

The research leading to these results has been performed within the STREAMS project (www.project-streams.eu) and received funding from

the European Community's Horizon 2020 program under Grant Agreement n° 688564.

References

[1] Heat Transfer Module User's Guide, COMSOL V5.2, 2015.

[2] M. Jaegle, "Simulating Thermoelectric Effects with Finite Element Analysis using COMSOL", Proceedings ECT, Odessa, p. 222, (2007).